27 May 2010, 7:30 pm - 9:00 pm

Investigation of Shear Strain Amplitude Induced by Railroad Traffic in Soils

Dirk Wegener
Engineering office GEPRO Ingenieurgesellschaft GmbH, Germany

Ivo Herle
Technische Universität Dresden, Institute of Geotechnical Engineering, Germany


Fifth International Conference on
Recent Advances in Geotechnical Earthquake Engineering and Soil Dynamics
and Symposium in Honor of Professor I.M. Idriss
May 24-29, 2010 • San Diego, California

INVESTIGATION OF SHEAR STRAIN AMPLITUDE INDUCED BY RAILROAD TRAFFIC IN SOILS

Dirk Wegener
Engineering office GEPRO Ingenieurgesellschaft GmbH
Caspar-David-Friedrich-Straße 8, 01219 Dresden, Germany

Ivo Herle
Technische Universität Dresden, Institute of Geotechnical Engineering
George-Bähr-Straße 1, 01062 Dresden, Germany

ABSTRACT

Shear strain amplitude γ is an important quantity in dynamic soil analysis. Usually, a reduction of soil stiffness with increasing shear strain amplitude is observed in laboratory tests. An appropriate invariant of shear strain can be defined which is comparable with shear strains measured in laboratory tests.
Usually, shear wave velocity c_s is determined from field or laboratory tests and the particle velocity v is obtained from vibration measurements. Afterwards, the shear strain amplitude γ is often estimated from the equation $\gamma = v / c_s$, which can be derived for the case of one dimensional wave propagation.
Based on numerical analyses with FEM, the validity of the above equation for γ is checked. It can be shown that there is a clear difference between the zone close to the loading area and the zone at a larger distance from the loading area.
Experimental results of vibration measurements in the field and the evaluation of dynamic soil properties due to rail traffic are presented and the impact on permanent soil deformations is discussed.
Based on the results of the field measurements and the numerical calculations recommendations on the determination of γ for dynamic analysis are presented.

INTRODUCTION

Shear strain amplitude γ is an important quantity in dynamic soil analysis. An increasing shear strain amplitude results in decreasing shear modulus, increasing damping and higher accumulation of plastic soil deformation due to repeated loading, e.g. by traffic forces.

Therefore, e.g. in the rules of the German Railways for earthworks RIL 836 [2008] for the proof of the so-called dynamic stability or serviceability, respectively, a comparison of actual shear strains with allowable shear strains is required. Also in case of dynamically loaded foundations it is necessary to identify the shear strain amplitude, see e.g. Savidis et. al. [2002].

In practise, the shear wave velocity c_s is usually determined from field tests and the particle velocity v is obtained from vibration measurements. Afterwards, the shear strain amplitude γ is often estimated from the equation $\gamma = v / c_s$, which can be derived for the case of one dimensional wave propagation, see e.g. Achenbach [1984].

In this paper, the validity of the equation $\gamma = v / c_s$ is investigated, using the results of field measurements and numerical calculations.

DEPENDENCE OF SHEAR MODULUS *G* ON SHEAR STRAIN γ

It can be observed in cyclic and dynamic laboratory tests that the stiffness of soil (shear modulus) decreases with increasing shear strain amplitude, with a maximum value of the shear modulus G_0 at very small strains.

In Vucetic [1994] and further in Hsu and Vucetic [2004] the magnitude of shear strain is classified on the basis of 16 laboratory test series on sands and clays. One can distinguish the following ranges:

- very low shear strain with linear elastic soil behaviour,
- low shear strain with nonlinear soil behaviour and

- medium to large shear strain with strongly nonlinear material behaviour.

The threshold between very low shear strain and low shear strain is called the linear cyclic threshold shear strain. The threshold between low shear strain and medium to large shear strain is called the volumetric cyclic threshold shear strain.

The test results show, in spite of a significant scatter, that in non-cohesive soils the nonlinear behaviour begins at a much lower shear strain γ than in soils with high plasticity.

For the evaluation of test results (Vucetic [1994], Hsu and Vucetic [2004]) it is important that 15 of 16 laboratory experiments were performed in a cyclic Direct Simple Shear (DSS). For the determination of the shear modulus $G(\gamma)$ as a function of shear strain γ, one should consider the shear strain component γ_{xy} defined in a Direct Simple Shear (see Figure 2).

DEFINITION OF SHEAR STRAIN γ

In three-dimensional coordinate system X_1, X_2 and X_3 the strain tensor ε_{ij} with 6 independent strain components can be defined: ε_{11}, ε_{22}, ε_{33}, γ_{12}, γ_{23} and γ_{31}.

The strain components ε_{ii} are $\varepsilon_{ii} = \partial u_i / \partial X_i$, and the shear strain components γ_{ij} are $\gamma_{ij} = 2\ \varepsilon_{ij} = \partial u_i / \partial X_j + \partial u_j / \partial X_i$ with indices i and j for the directions *1*, *2* and *3*.
The strain tensor ε_{ij} can be decomposed in isotropic strain tensor $\varepsilon_v/3\ \delta_{ij}$ and in a deviatoric strain tensor e_{ij}:

$$\varepsilon_{ij} = \varepsilon_v/3\ \delta_{ij} + e_{ij} \qquad (1)$$

with the Kronecker symbol δ_{ij} ($\delta_{ij} = 1$ for $i = j$ and $\delta_{ij} = 0$ for $i \neq j$) and the volumetric strain ε_v ($\varepsilon_v = \varepsilon_{11} + \varepsilon_{22} + \varepsilon_{33}$).

Figure 1 shows a total displacement and its decomposition in isotropic and deviatoric part. The isotropic part results in volumetric strains and the deviatoric part results in shear strains.

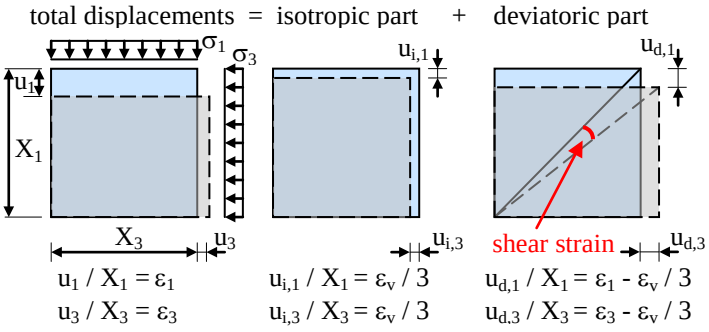

Fig. 1. Total displacement and decomposition in isotropic and deviatoric part in a plane with $u_2 = 0$.

Since the strain components depend on rotation of the coordinate system, it is necessary to define an invariant of the deviatoric strain tensor e_{ij} which characterises shear strain. For this purpose the second invariant II_e of the deviatoric strain tensor e_{ij} will be used. Considering the principal strain components ε_1, ε_2 and ε_3 one gets:

$$II_e = 1/2\ e_{ij}\ e_{ij} = 1/6\ [(\varepsilon_1 - \varepsilon_2)^2 + (\varepsilon_2 - \varepsilon_3)^2 + (\varepsilon_3 - \varepsilon_1)^2] \qquad (2)$$

In triaxial compression $\varepsilon_1 > \varepsilon_2 = \varepsilon_3$, $\varepsilon_v = \varepsilon_1 + 2 \cdot \varepsilon_3$ and $II_e = 1/3\ (\varepsilon_1 - \varepsilon_3)^2$ hold.

In a direct simple shear test, a relative horizontal displacement u_x between the top and the bottom cap is produced. The ratio u_x / Y corresponds to the shear strain γ_{xy} with plane strain conditions ($\gamma_{yz} = \gamma_{zx} = \varepsilon_{zz} = 0$), see Figure 2.

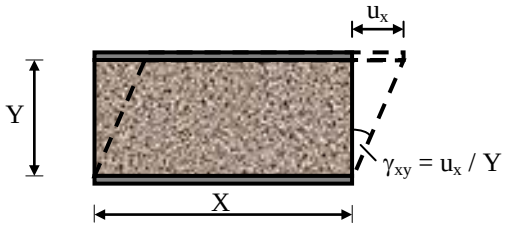

Fig. 2. Direct Simple Shear test with a constant volume.

With the assumption of vanishing vertical displacements during shearing ($\varepsilon_{yy} = u_y / Y \approx 0$), which can be assumed for small strains, three principal strain components read as follows:

$$\varepsilon_1 = 1/2\ \gamma_{xy},\ \varepsilon_2 = 0 \text{ and } \varepsilon_3 = -1/2\ \gamma_{xy}.$$

In this case, the second invariant of the deviatoric strain tensor e_{ij} in simple shear corresponds to: $II_e = 1/4\ \gamma_{xy}^2$.

The shear strain invariant γ corresponding to the shear strain component γ_{xy} in simple shear can be obtained from equation (2) as:

$$\gamma = \gamma_{xy} = 2\ II_e^{0.5} = (2/3)^{0.5}\ [(\varepsilon_1 - \varepsilon_2)^2 + (\varepsilon_2 - \varepsilon_3)^2 + (\varepsilon_3 - \varepsilon_1)^2]^{0.5} \qquad (3)$$

By rotating the coordinate system it is possible to achieve strain conditions like in a simple shear test.

NUMERICAL ANALYSIS OF WAVE PROPAGATION IN ELASTIC HALFSPACE AND IN LAYERED SOIL

Using numerical methods one can calculate the shear strain invariant γ at any point in subsoil.
In practice, the particle velocity v is measured using geophones or obtained by time integration from accelerometers. Then the shear strain is usually calculated from the equation $\gamma = v / c_s$, see e.g. Savidis et. al. [2002] for dynamically loaded foundations or Hu et al. [2003] for evaluating the dynamic stability of railway earthworks.

Based on numerical analyses with FEM, the validity of the equation for γ is checked for case of wave propagation in elastic halfspace and in layered soil.

Numerical model

An axisymmetric FE model with elastic material (constant Young's modulus) and with the boundary conditions shown in Figure 3 is assumed.

The FE program *Tochnog* (Roddemann [2008]) with the following material properties is applied:

- Young's modulus $E = 50$ or 100 MPa,
- Poisson's ratio $\nu = 0.30$ and
- density $\rho = 2.0$ t/m^3.

Material damping is not considered.

The size of the FE model in the horizontal direction is chosen so that reflections of shear and Rayleigh waves at the horizontal boundary do not affect the results at the regarded points near the loading area.

The loading is located on the surface having the loading sequence of a sine wave of *5*, *10* and *20* Hz with an amplitude of 10 kPa and subsequently stress-free surface (see Figure 4 top left).
This is not a period harmonic excitation, thus no single line is obtained in the frequency spectrum but a curve with a maximum at about *4.5*, *9.0* and *18* Hz, see the diagram in the upper right corner of Figure 3.
The time step $\Delta t = 0.0025$ s was used in order to capture well the sine wave with *20* Hz. With the chosen element size and the node distance $l_c = 0.25$ m $\leq c_s \cdot \Delta t = 138.7$ m/s $\cdot$ *0.0025* s $= 0.35$ m, the wave propagation within the mesh can be sufficiently reproduced.

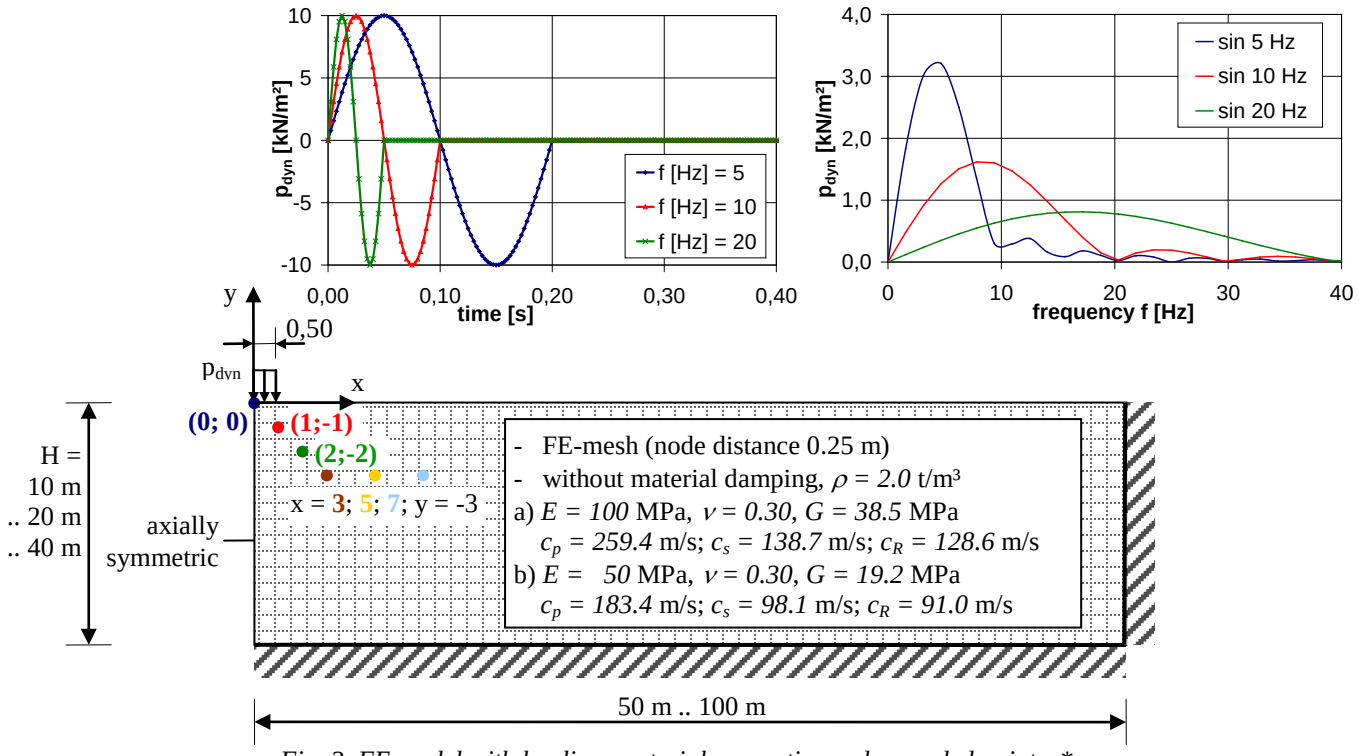

*Fig. 3. FE model with loading, material properties and regarded points. **

* The coordinates of the regarded points are in meters. In the subsequent text and in Figures the units are omitted for the sake of brevity.

Displacements

In Figure 4, vertical displacements are shown in time domain for the regarded points ($x = 1, y = -1$) and ($x = 5, y = -3$). The amplitudes of vertical displacement at the point ($x = 1, y = -1$) near to the loading area are approximately the same for all load frequencies. However, for the point ($x = 5, y = -3$) in a larger distance from the loading area, the amplitudes of vertical displacement are slightly greater for *5* Hz than for *10* Hz and significantly larger than for *20* Hz.

In frequency domain the differences in displacements between the zone close to the loading area and the zone at a larger distance from the loading area are also remarkable.

For a soil layer with a thickness H and the compression wave velocity c_p its natural frequency f_E can be obtained from equation (4) (see Neidhart [1994]).

$$f_E = c_p / (4\,H) \tag{4}$$

A peak of the vertical displacement can be noticed in Figure 5 at the natural frequency f_E for the point ($x = 5, y = -3$) at the largest distance from the loading area (green curve).
However, for the point ($x = 0, y = 0$) on the surface below the loading area (blue curve) such a peak at the natural frequency f_E is missing. The curve reaches its maximum at about 9.0 Hz and is qualitatively analogous to the shape of the loading curve for a sine wave of 10 Hz shown in Figure 3, top right.

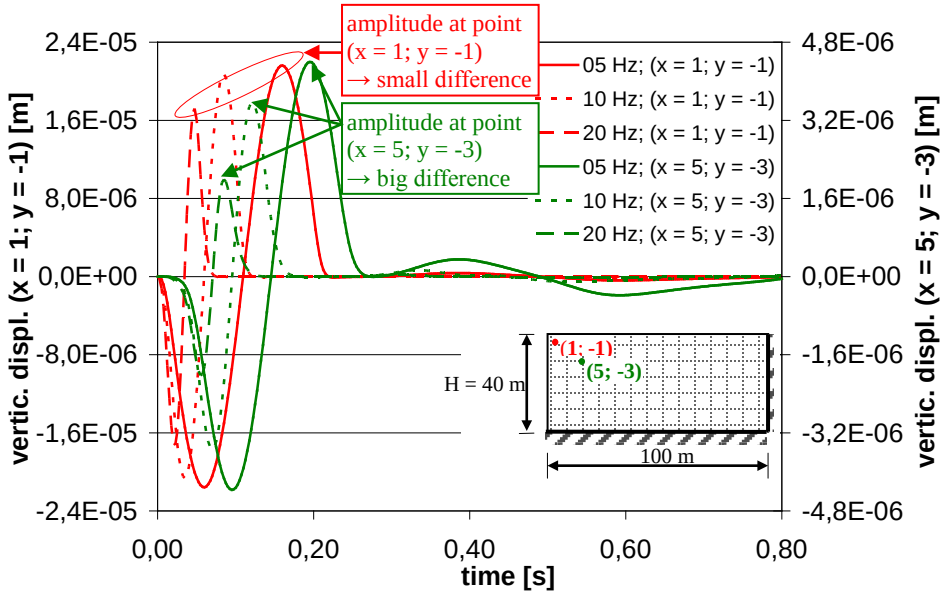

Fig. 4. Vertical displacements in time domain at loading of 5, 10 and 20 Hz for the points (x = 1, y = -1) and (x = 5, y = -3).

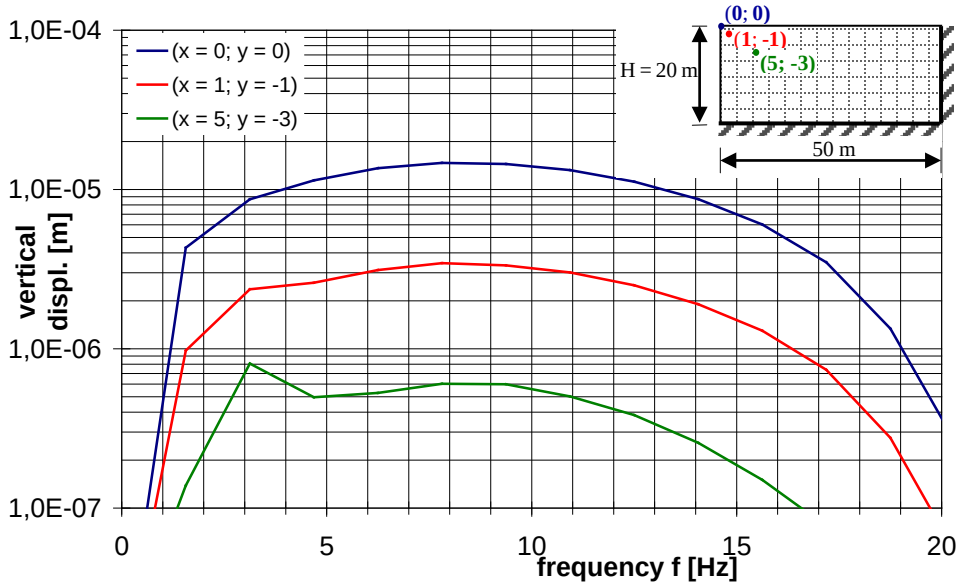

Fig. 5. Vertical displacements in frequency domain at loading of 10 Hz for the points (x = 0, y = 0); (x = 1, y = -1); (x = 5, y = -3).

For the point ($x = 1$, $y = -1$) near to the loading area (red curve) a peak at the natural frequency f_E of the soil layer is slightly indicated, but less significantly than at the point ($x = 5$, $y = -3$), see the green curve. The shape of the red curve is again similar to the loading curve for a sine wave of *10* Hz shown in Figure 3, top right.

The influence of different thickness and of Young's modulus was also investigated. Three different cases were considered:

- $H = 10$ m; $E = 100$ MPa; $\nu = 0.30$; $E_s = 134.6$ MPa; $c_p = 259.4$ m/s (blue curve): $f_E \approx 6.5$ Hz,
- $H = 10$ m; $E = 50$ MPa; $\nu = 0.30$; $E_s = 67.3$ MPa; $c_p = 183.4$ m/s (green curve): $f_E \approx 4.6$ Hz and
- $H = 20$ m; $E = 100$ MPa; $\nu = 0.30$; $E_s = 134.6$ MPa; $c_p = 259.4$ m/s (red curve): $f_E \approx 3.25$ Hz.

The calculated vertical displacement in frequency domain at the point ($x = 5$, $y = -3$) at a large distance from the loading area is depicted in Figure 6. Peaks of the vertical displacement at the natural frequencies f_E are clearly visible.

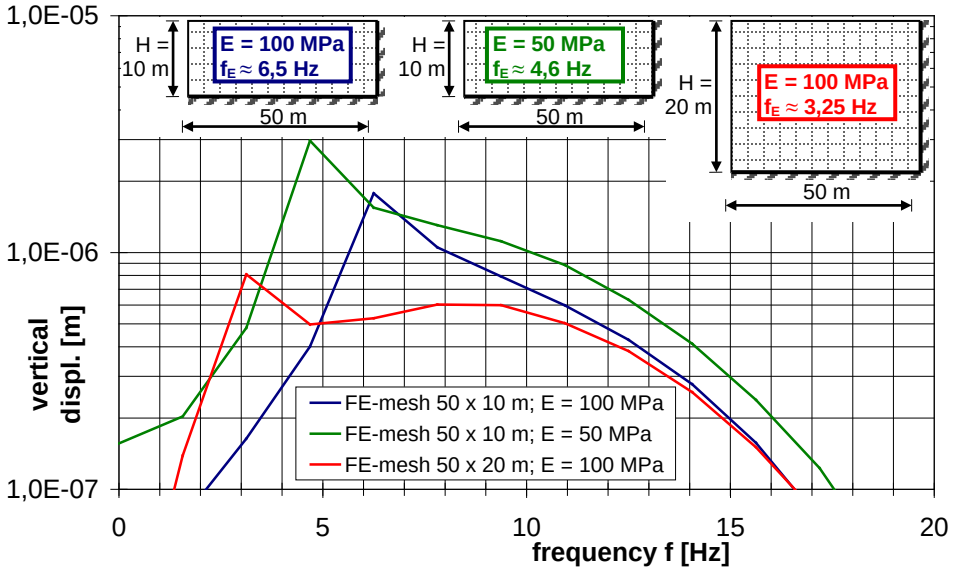

Fig. 6. Vertical displacements in frequency domain at loading of 10 Hz for the point ($x = 5$, $y = -3$).

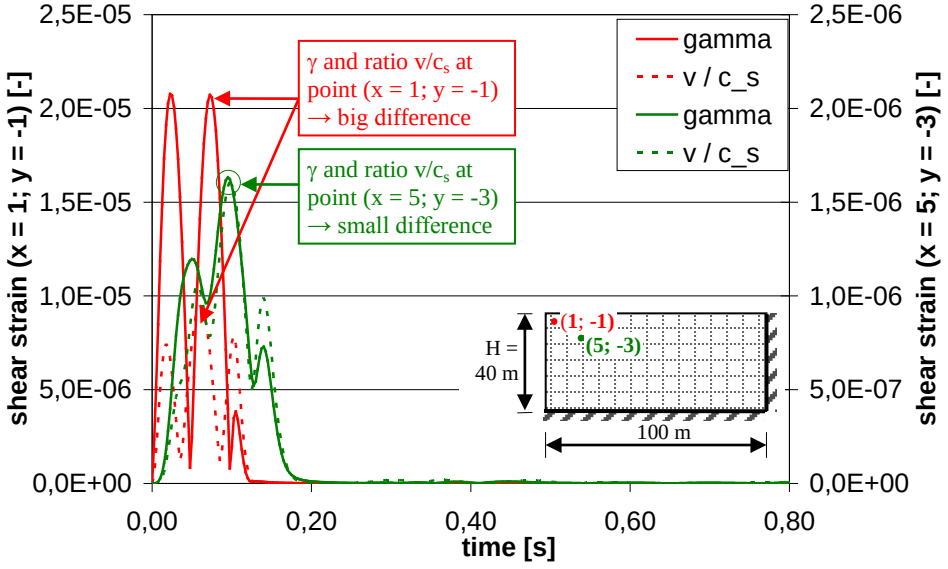

Fig. 7. Comparison of shear strain γ and the ratio v / c_s at loading 10 Hz for the points ($x = 1$, $y = -1$); ($x = 5$, $y = -3$).

Shear strain

Similar to the displacements, shear strains in a near and in a distant zone to the loading area can be calculated. They can be compared with the ratio of vibration velocity v and shear wave velocity c_s (see Figure 7).

There is a big difference between γ and v / c_s in the area close to the loading (in this example for the point ($x = 1$, $y = -1$), red curve). There, the shear strain γ is much larger than the ratio v / c_s.
In a larger distance from the loading area (in this example at the point ($x = 5$, $y = -3$), green curve) the shear strain γ is approximately the same as the ratio v / c_s.

These differences between the zone close to the loading area and the zone at a larger distance from the loading area are significant also at loading of *5* Hz and *20* Hz. However, with increasing excitation frequency the zone area decreases, where γ and the ratio v / c_s are significantly different.

EXPERIMENTAL RESULTS OF VIBRATION MESUREMENTS

Railway line in North Germany

On a railway line section in North Germany a single-track superstructure and substructure required rehabilitation. An increase of speed to 160 km/h was planed. The original track construction from the 19th century was founded on a marshy ground overbuild with an embankment.
In some sections of the railway line the improvement was achieved by including a geotextile reinforced base layer instead of the originally planed extensive improvement [12].
During the rehabilitation construction works a cross section (Figure 8) was instrumented with geophones and with a horizontal inclinometer in the subsoil.

The results of the geophysical measurements of shear wave velocity can be summarized as follows:

- sandy embankment: $c_s \approx 160$ m/s,
- peat beside the embankment (free field): $c_s \approx 50$ m/s,
- peaty clay beside the embankment (free field): $c_s \approx 70$ m/s,
- peat below the embankment $c_s \approx 100$ m/s and
- peaty clay below the embankment $c_s \approx 120$ m/s.

An example for the measured particle velocity in the subsoil is shown in Figure 8. The displacements were obtained by time-integration of the measured particle velocity in Figure 9.

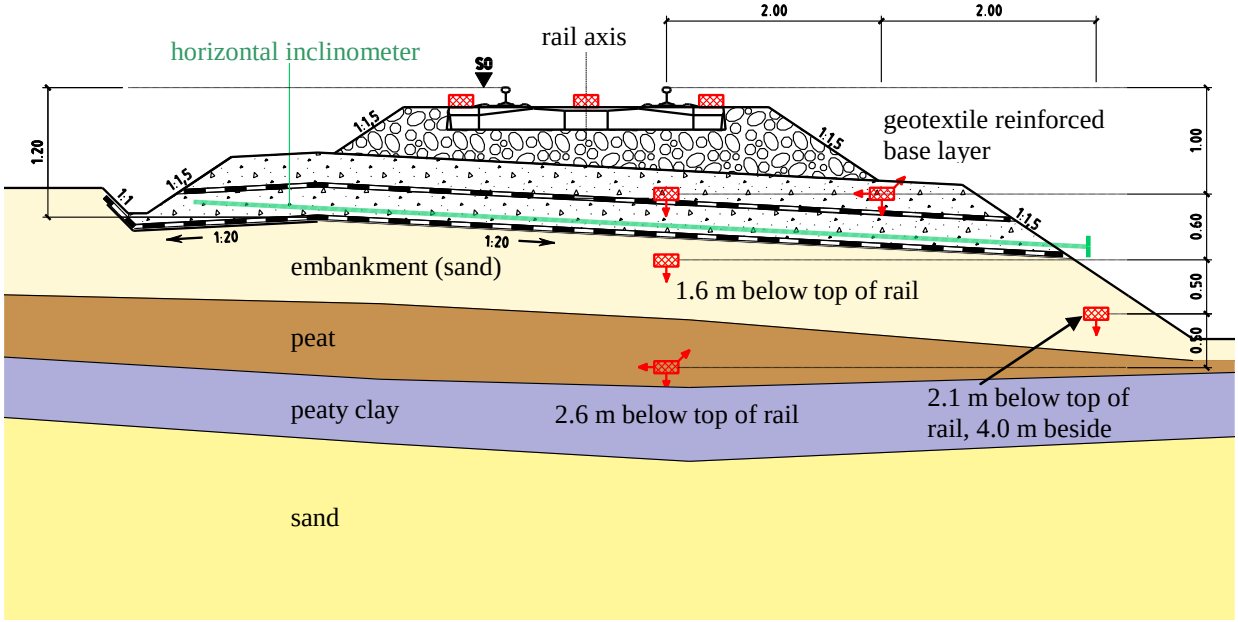

Fig. 8. Cross section with instrumentation of geophones and horizontal inclinometer.

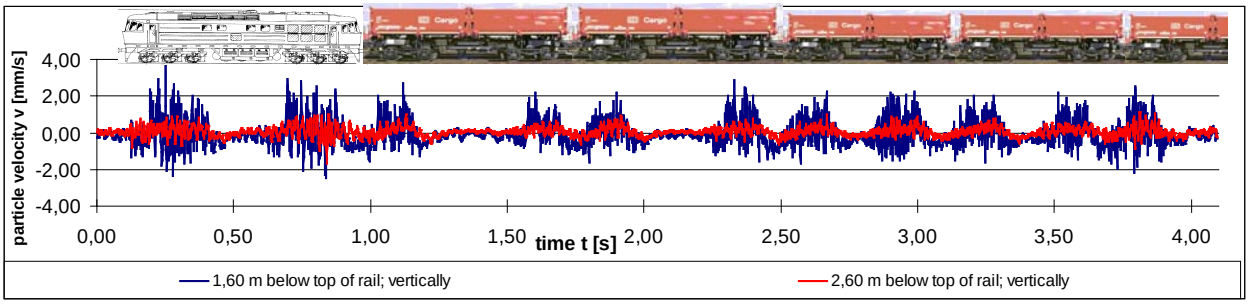

Fig. 9. Measured particle velocity during the train passage.

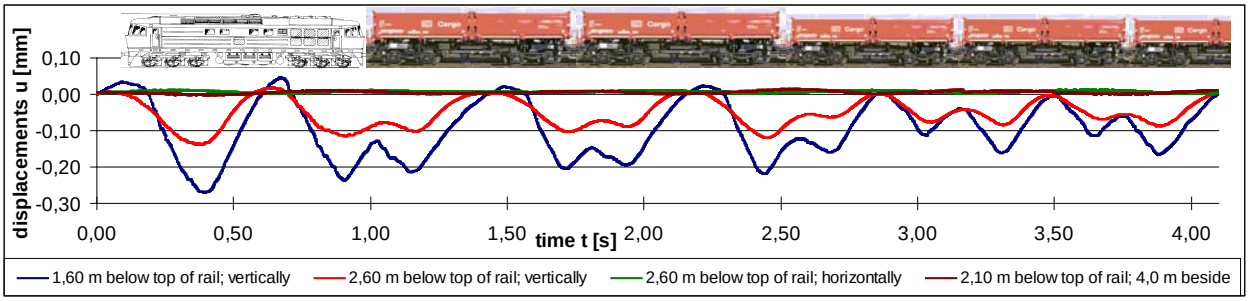

Fig. 10. Calculated particle displacements during the train passage.

From the displacements below the rail one can estimate an average shear strain in this subsoil zone (see Figure 11).

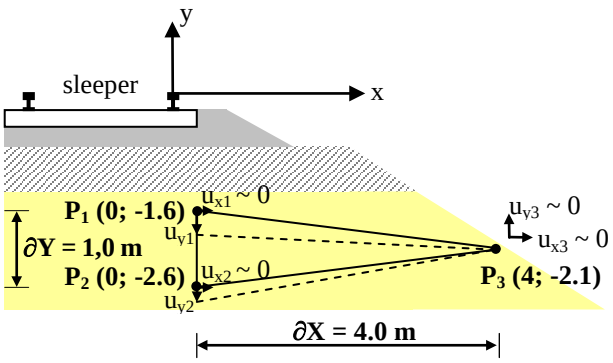

Fig. 11. Estimation of the average shear strain at the depth between 1.6 m and 2.6 m below the top of the rail.

The average strain components in x- and y-direction ε_{xx} and ε_{yy} and the shear strain γ_{xy} within the area ∂X and ∂Y can be calculated as:

$$\varepsilon_{xx} = \partial u_x / \partial X \approx [u_{x2} - u_{x3}] / \partial X ,$$
$$\varepsilon_{yy} = \partial u_y / \partial Y \approx [(u_{y1} - u_{y2}) / 2 + u_{y3}] / \partial Y \text{ and}$$
$$\gamma_{xy} = \partial u_x / \partial Y + \partial u_y / \partial X \approx 0 + [u_{y3} - (u_{y1} + u_{y2}) / 2] / \partial X .$$

This calculation is a crude estimation only, since strains are infinitesimal quantities. Using the strain components ε_{xx}, ε_{yy} and γ_{xy}, one can calculate the principal strains ε_1 and ε_3 and the shear strain invariant γ for the whole time period of the train passage.

In Figure 12 a comparison of the shear strain invariant γ with the ratio of the particle velocity $v_{res} = (v_x^2 + v_y^2 + v_z^2)^{1/2}$ and the shear wave velocity c_s is presented.

One can notice that the shear strain magnitude γ is much higher than the ratio v_{res} / c_s. The highest shear strain magnitude γ is about *9.5E-5* under the 3-axle bogie locomotive and is nearly proportional to the vertical displacements (Figure 10). The highest ratio v_{res} / c_s is about *3.0E-5* and it is proportional to the measured particle velocity (see Figure 9).

After the rehabilitation of this railway line section, permanent displacements in the instrumented cross section were measured over a period of two years [13]. The results are depicted in Figures 13 and 14.

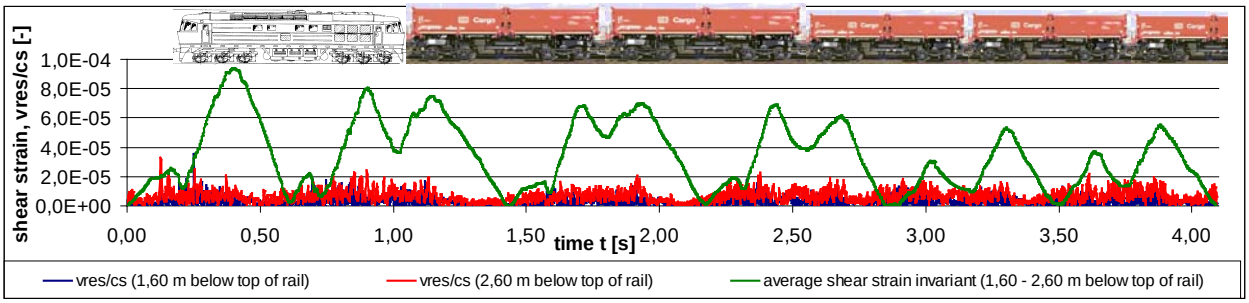

Fig. 12. Comparison of the shear strain invariant γ with the ratio v_{res} / c_s.

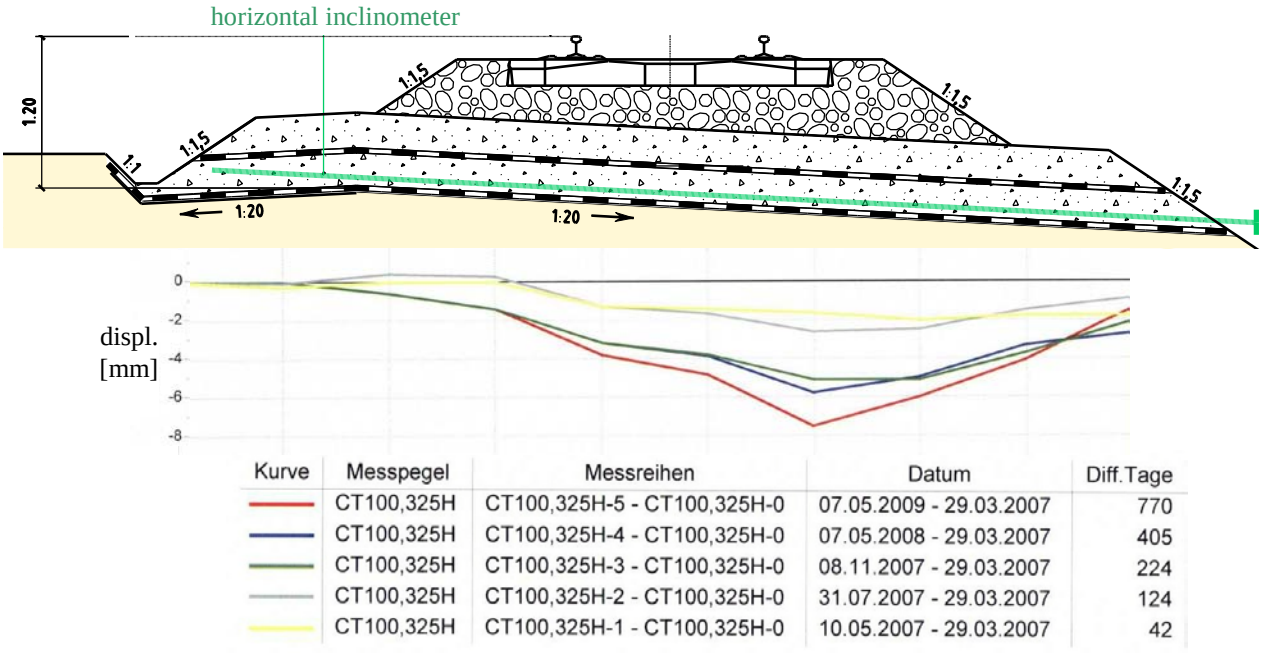

Fig. 13. Cross section with results of the horizontal inclinometer measurements.

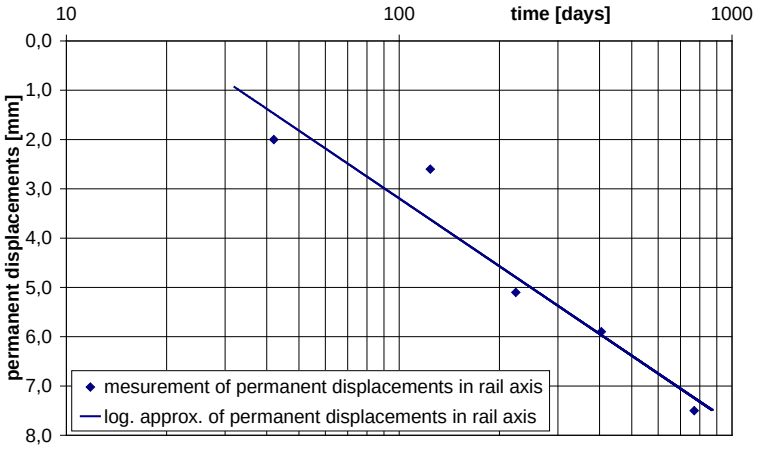

Fig. 14. Inclinometer measurements of permanent displacements in the subsoil.

One can notice that the traffic with dynamic loading of about 280 cycles per day or 100.000 cycles per year results in permanent displacements. It is obvious that the magnitude γ is greater than the threshold cyclic shear strain $\gamma_{tv} \approx 8E\text{-}5$ for the subsoil with $I_P \approx 0$ as defined in Hsu and Vucetic [2004]. But the increase of permanent displacements reduces nearly logarithmically with time and the number of cycles, respectively.

Railway line in South Germany

On a railway line section in South Germany a double-track superstructure and substructure were also founded on a very marshy ground with about *1.5* m soft clay and about *3.0* m peat.
Before rehabilitation of the railway line the cross section was instrumented with geophones and down-hole tests were carried out to obtain the shear and compression wave velocities (see Figure 15).

The results of the measurements can be summarized as follows:

- clayey gravel below the rail track: $c_s \approx 130$ m/s,
- soft clay below the clayey gravel: $c_s \approx 110$ m/s
- peat below the soft clay: $c_s \approx 90$ m/s.

The shear wave velocity in the transition zone between ballast and clayey gravel (*0.5* m below the top of sleepers) was estimated as $c_s \approx 160$ m/s.

Geophones (SM 6, 4.5 Hz) were placed on the sleeper, in the ballast and in the subsoil. Thus it was possible to measure particle velocity (Figure 16) and to obtain the displacements by time-integration of the measured particle velocity (Figure 17). From the displacements below the sleeper one can calculate an average shear strain in the zone of the clayey gravel (see Figure 18) and also in the zone of soft clay and peat (see Figure 19).

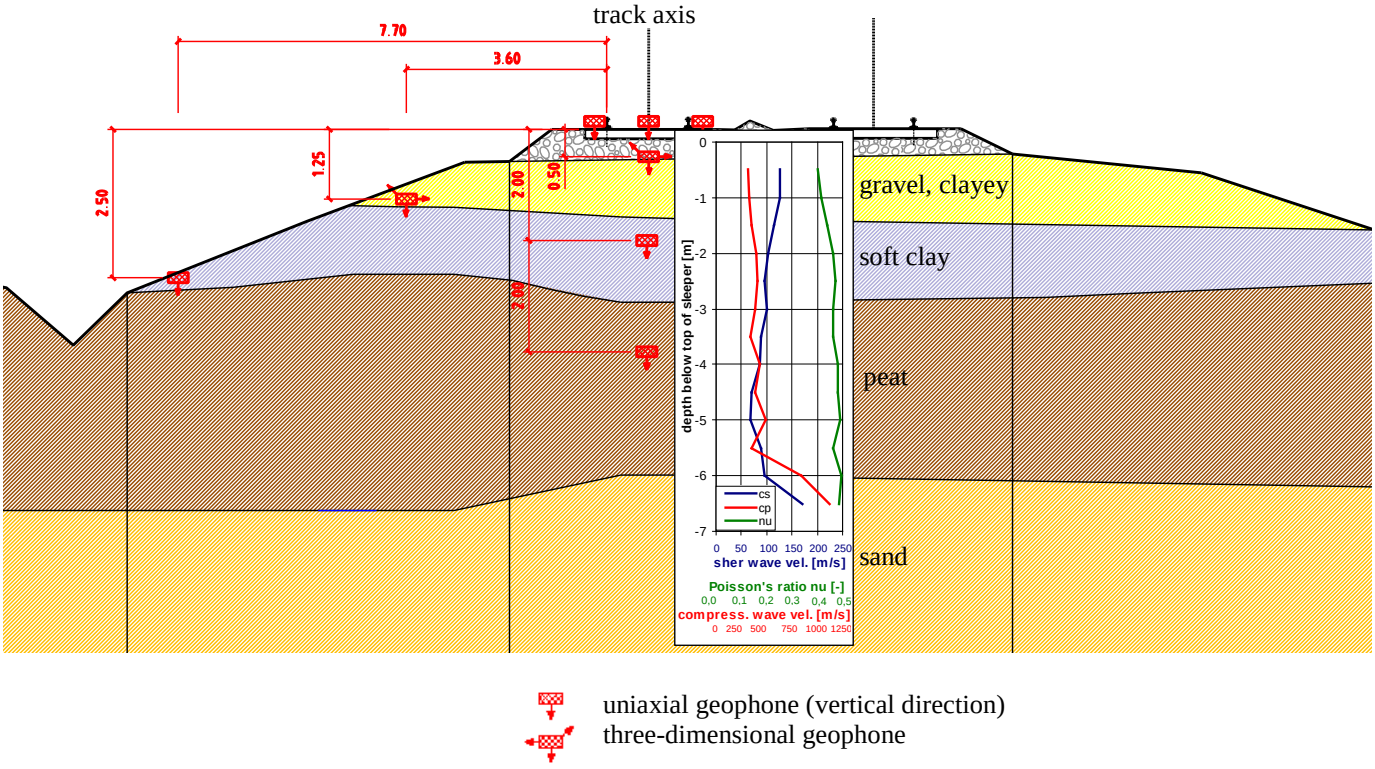

Fig. 15. Cross section with instrumentation of geophones and results from down-hole tests.

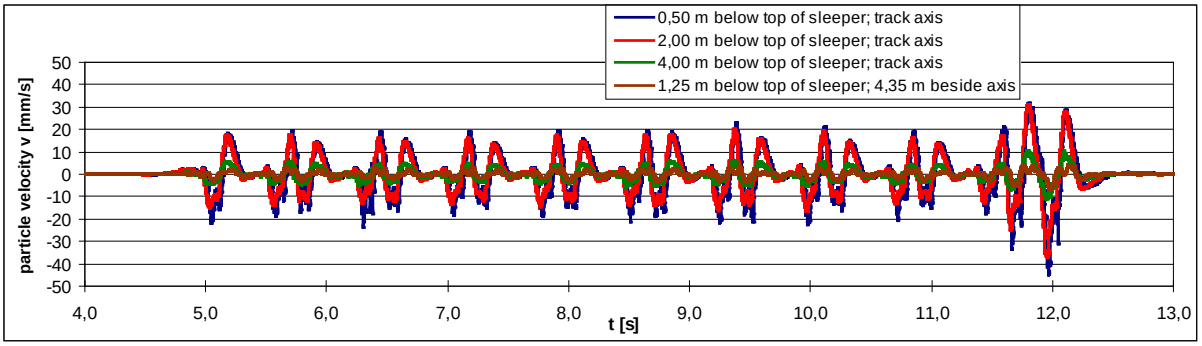

Fig. 16. Measured particle velocity during the train passage.

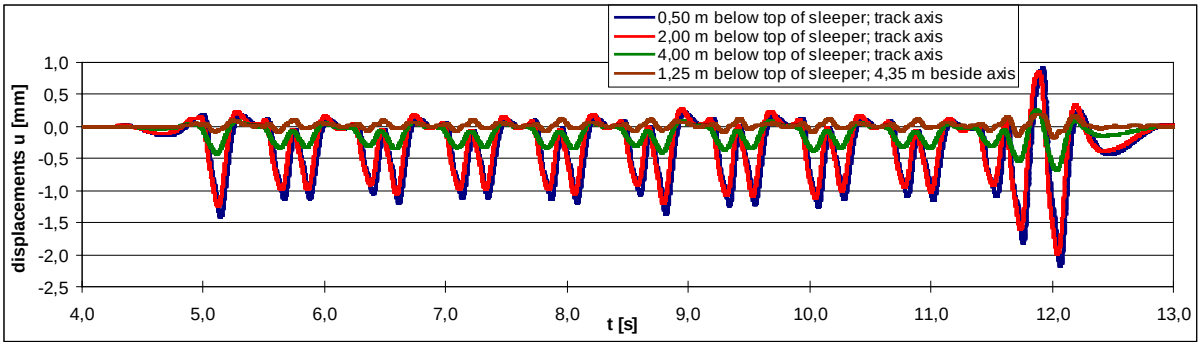

Fig. 17. Calculated particle displacements during the train passage.

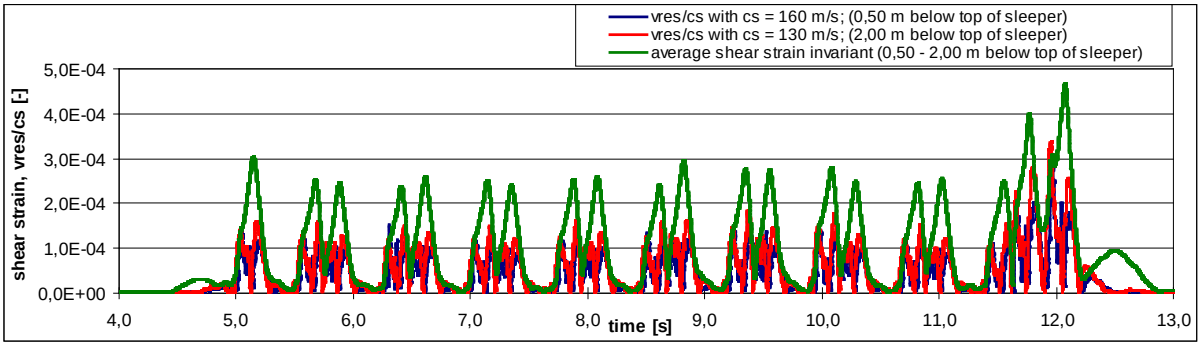

Fig. 18. Comparison of the shear strain invariant γ with the ratio v_{res} / c_s in area of the clayey gravel.

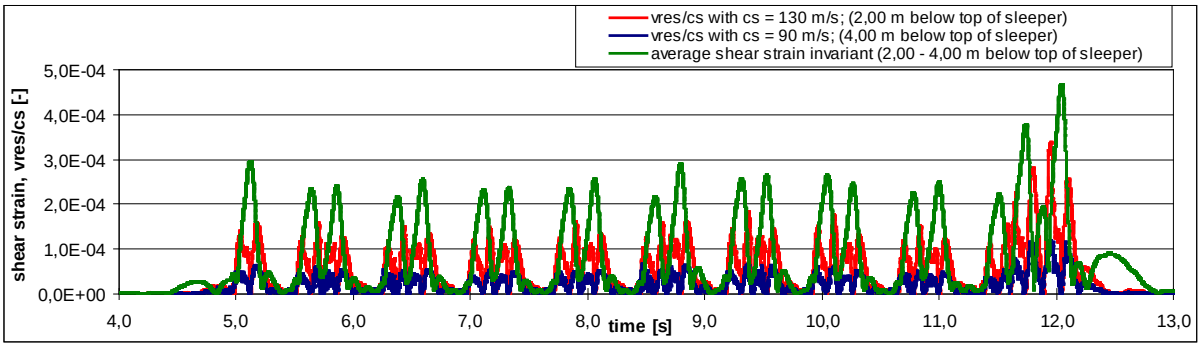

Fig. 19. Comparison of the shear strain invariant γ with the ratio v_{res} / c_s in area of soft clay and peat.

The average shear strain invariants in the clayey gravel, in the soft clay and in the peat are nearly the same. In the soft clay and in the peat the strain component in vertical direction $\varepsilon_{yy} = \partial u_y / \partial Y$ is higher, but the shear strain $\gamma_{xy} \approx \partial u_y / \partial X$ is lower than in the clayey gravel.

One can notice that the shear strain magnitude γ is significantly higher than the ratio v_{res} / c_s. The highest shear strain magnitude γ is nearly proportional to the vertical displacements with maximum about *4.6E-4* (Figure 18). The highest ratio v_{res} / c_s is about *2.8E-4* in the transition zone between the ballast and the clayey gravel (*0.5* m below the top of the sleeper); *3.3E-4* in the soft clay (*2* m below the top of the sleeper) and *1.2E-4* in the peat (*4* m below the top of the sleeper).
The shear strain magnitude γ is much larger than the threshold cyclic shear strain $\gamma_{tv} \approx$ *1.3E-4* for the clayey gravel with $I_P \approx$ *10* and $\gamma_{tv} \approx$ *2.8E-4* for the soft clay with $I_P \approx$ *25 - 30* according to Hsu and Vucetic [2004].
Thus it can be assumed that the permanent displacements due to dynamic loading of about 1.000 cycles per day or nearly 400.000 cycles per year do not increase logarithmically but nearly linearly with time and the number of cycles, respectively. At this railway line section it is necessary to tamp the ballast about once a year.

CONCLUDING REMARKS

It can be observed that there is a clear difference in the soil behaviour in the zone close to the loading area and in the zone at a large distance from the loading area.

In the zone close to the loading area displacements and hence shear strains depend mainly on excitation characteristics. Soil undergoes cyclic loading conditions and inertia effects of the soil mass do not play an important role for the wave propagation. However, at a larger distance from the loaded area energy dissipation during the wave propagation in soil (radiation damping) becomes significant.
Figure 20 shows schematically the load in the zone close and in a larger distance to the loading area.

In a larger distance from the loading area Rayleigh waves with the velocity c_r dominate near to the surface. Rayleigh wave velocity c_r is only slightly lower than the shear wave velocity c_s and the compression waves have much lower vibration amplitude. Therefore, by rotating the coordinate system (see Figure 20) the plane wave propagation becomes nearly a one-dimensional wave propagation. The maximum vibration amplitude is perpendicular to the wave propagation direction. The following equation is valid:

$$\gamma = \gamma_{xy} = \partial u_x / \partial Y + \partial u_y / \partial X \approx \partial u / \partial t / c_s = v / c_s \qquad (4)$$

In a three-dimensional case, especially if the compression waves have more influence like in tunnelling, this relationship does not valid. Here, general equations for strains and displacements as function of c_s and c_p should be used, see e.g. Kolymbas [2005].

In the zone close to the loading area, which has the largest potential for permanent deformations due to dynamic loading, soil undergoes almost cyclic loading conditions like in a cyclic simple shear or cyclic triaxial test. Thus, for example, doubling the loading frequency results in a doubled particle velocity, while the shear strain amplitude remains the same. Consequently, the equation $\gamma \approx v / c_s$ can not be applied in this area.

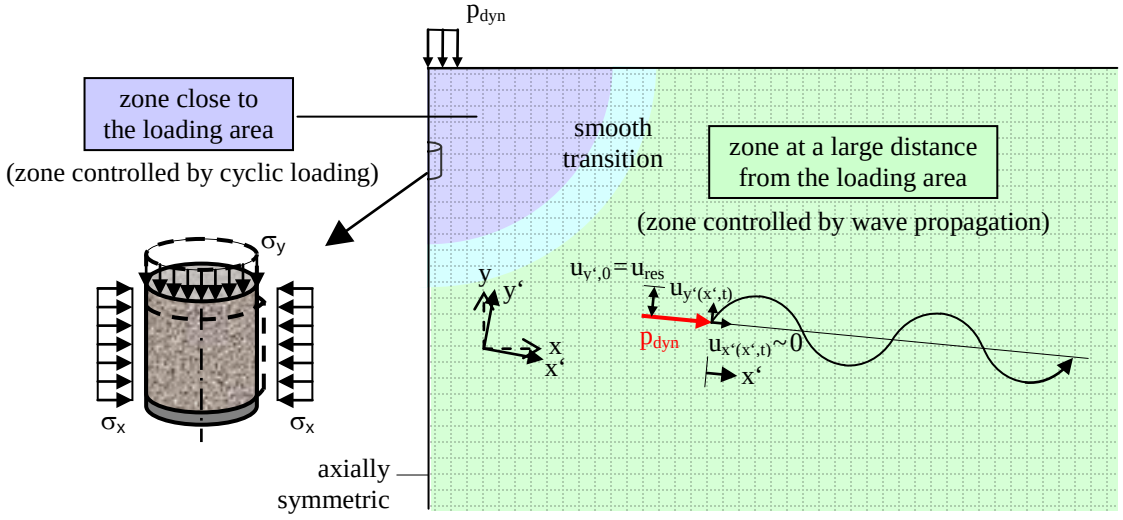

Fig. 20. Schematic representation of the conditions in the close and distant zones with respect to the loading area.

REFERENCES

Achenbach, J.D. [1984]. "*Wave propagation in elastic solids*". Vol. 16. North-Holland series in applied mathematics and mechanics.

Savidis, S. et. al. (ed.) [2002]. „*Empfehlungen des Arbeitskreises 1.4 Baugrunddynamik der DGGT*". Berlin: Deutsche Gesellschaft für Geotechnik.

Hsu, C. C. and Vucetic, M. [2004]. "*Volumetric threshold shear strain for cyclic settlement*". ASCE, Journal of Geotechnical and Geoenvironmental Engineering Vol. 130, No.1, pp. 58-70.

Hu, Y. et. al. [2002]. „*Bewertung der dynamischen Stabilität von Erdbauwerken unter Eisenbahnverkehr*". Geotechnik Vol. 26, No.1, pp. 42-56.

Kolymbas, D. [2005]. „*Tunnelling and Tunnel Mechanics*". Berlin, Heidelberg: Springer Verlag.

Neidhart, T. [1994]. „*Lösung dreidimensionaler linearer Probleme der Bodendynamik mit der Randelementmethode*". PhD thesis. No. 131, University Fridericiana Karlsruhe.

RIL 836 [2008]. „*Richtlinie 836: Erdbauwerke und sonstige geotechnische Bauwerke planen, bauen und instand halten*". German Railway network Inc.

Roddemann, D. [2008]: „*TOCHNOG Professional Version 4.3*". URL: http://www.feat.nl.

Vucetic, M. [1994]. "*Cyclic threshold shear strains in soils*". ASCE, Journal of Geotechnical and Geoenvironmental Engineering vol. 120, No.12, pp. 2008-2227.

Wegener, D., U. Weisemann, T. Neidhart and G. Neumann [2008]. „*Ertüchtigung von Eisenbahnstrecken auf Weichschichten*". Der Eisenbahningenieur (59) No. 12.

Weisemann, U., R. Kipper, D. Wegener and G. Neumann [2009]. „*Messtechnische Begleitung der Sanierungsstrecke Casekow – Tantow*". 6. Geokunststoff-Kolloquium Naue.